Finite Volume Methods to extract Resonances

Michael Döring

Helmholtz-Institut für Strahlen- und Kernphysik, Universität Bonn

Bethe Center for Theoretical Physics

in collaboration with J. Haidenbauer, U.-G. Meißner, E. Oset, A. Rusetsky

INT 12-2b, Lattice QCD Studies of Excited Resonances and Multi-Hadron Systems
Institute for Nuclear Theory, Seattle WA, USA,
August 17, 2012

The simple cubic lattice

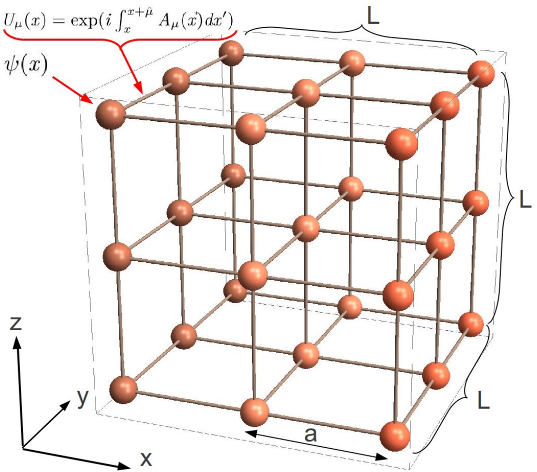

- Side length L, $V = L^3$ $(+L_t)$, periodic boundary conditions $\Psi(x) \stackrel{!}{=} \Psi(x + \hat{\mathbf{e}}_i L)$
  $\rightarrow$ finite volume effects
  $\rightarrow$ Infinite volume $L \rightarrow \infty$ extrapolation
- Lattice spacing a
  $\rightarrow$ finite size effects
  Modern lattice calculations: $a \simeq 0.07$ fm $\rightarrow p \sim 2.8$ GeV
  $\rightarrow$ (much) larger than typical hadronic scales;

  not considered here.
- Unphysically large quark/hadron masses
  $\rightarrow$ chiral extrapolation required.

Notation (I)
Scattering in the infinite volume limit

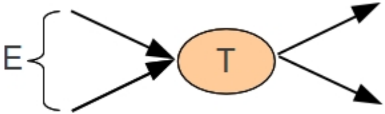

- $\rightarrow$ Generic (Lippman-Schwinger) equation for unitarizing the T-matrix:

$$T = V + V\,G\,T$$

  V: (Pseudo)potential

- G: Green's function:

$$\begin{aligned} G &= \int \frac{d^3\vec{q}}{(2\pi)^3} \frac{f(|\vec{q}|)}{E^2 - (\omega_1+\omega_2)^2 + i\epsilon}, \\ \omega_{1,2}^2 &= m_{1,2}^2 + \vec{q}^{\;2} \end{aligned}$$

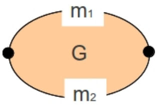

Notation (II)

Discretized momenta in the finite volume with periodic boundary conditions

$$\Psi(x) \stackrel{!}{=} \Psi(x + \hat{\mathbf{e}}_i\, L) = \exp\left(i\, L\, q_i\right) \Psi(x) \quad \Longrightarrow \quad q_i = \frac{2\pi}{L}\, n_i, \quad n_i \in \mathbb{Z}, \quad i = 1, 2, 3$$

$$\boxed{\int \frac{d^3 \vec{q}}{(2\pi)^3}\, g(|\vec{q}\,|^2) \to \frac{1}{L^3} \sum_{\vec{n}} g(|\vec{q}|^2), \quad \vec{q} = \frac{2\pi}{L}\, \vec{n}, \quad \vec{n} \in \mathbb{Z}^3}$$

$$G \to \tilde{G} = \frac{1}{L^3} \sum_{\vec{q}} \frac{f(|\vec{q}|)}{E^2 - (\omega_1 + \omega_2)^2}$$

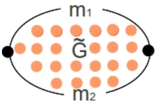

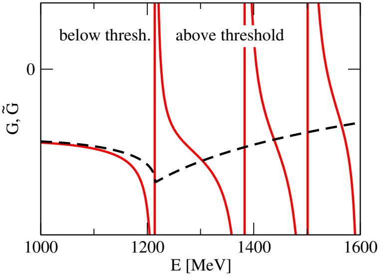

- $E > m_1 + m_2$: $\tilde{G}$ has poles at *free energies in the box*, $E = \omega_1 + \omega_2$
- $E < m_1 + m_2$: $\tilde{G} \to G$ exponentially with L (regular summation theorem).
- Here & following: formalism can be mapped to Lüscher's $\mathcal{Z}_{\ell m}$.

Notation (III)

- Poles of $\tilde{T}$ give the eigenvalues of the Hamiltonian (tower of *lattice levels* $E(L)$):

$$\tilde{T} = (1 - V\tilde{G})^{-1} V \;\rightarrow\quad V^{-1} - \tilde{G} \overset{!}{=} 0 \;\rightarrow\; V^{-1} = \tilde{G}$$

- The interaction V determines the T-matrix in the infinite volume limit:

$$T = \left(V^{-1} - G\right)^{-1} = \left(\tilde{G} - G\right)^{-1}$$

- Re-derivation of Lüscher's equation (T determines the phase shift δ):

$$\boxed{p\cot\delta(p) = -8\pi\sqrt{s}\left(\tilde{G}(E) - \mathrm{Re}\,G(E)\right)}$$

- V and dependence on renormalization have disappeared (!)

L-dependence of lattice levels

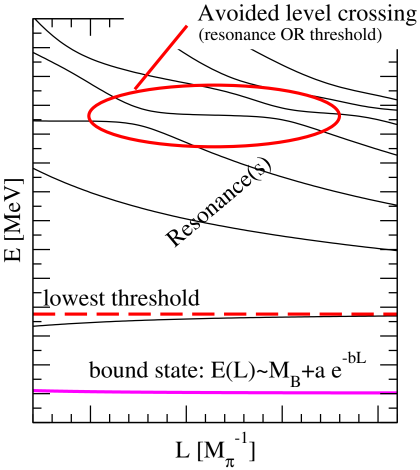

- L-dependence serves to extract phase shifts (Lüscher).
- ...for a narrow window in $E < \Gamma_{\sigma(600)}$.
- ... at the cost of several required lattice volumes.
- $\to$ Stabilize the phase extraction using model-independent information from Chiral Perturbation Theory.
- $\to$ Continuity assumption on the amplitude in combination with error analysis.

L-dependence of lattice levels

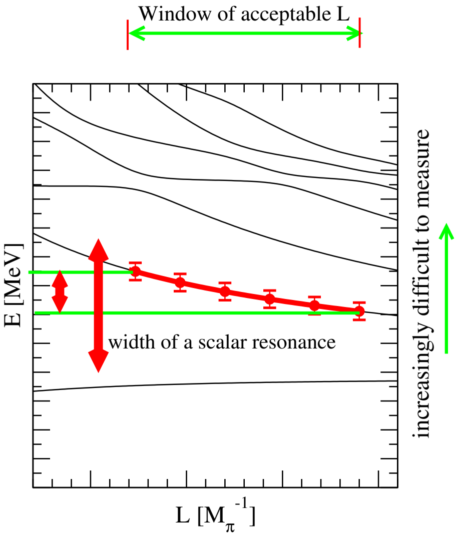

- L-dependence serves to extract phase shifts (Lüscher).
- ...for a narrow window in $E < \Gamma_{\sigma(600)}$.
- ... at the cost of several required lattice volumes.
- $\rightarrow$ Stabilize the phase extraction using model-independent information from Chiral Perturbation Theory.
- $\rightarrow$ Continuity assumption on the amplitude in combination with error analysis.

Synthetic lattice data from Unitarized ChPT

[M.D., Ulf-G. Meißner, JHEP **1201** (2012), using Inverse Amplitude Method (Pelaez *et al.*)]

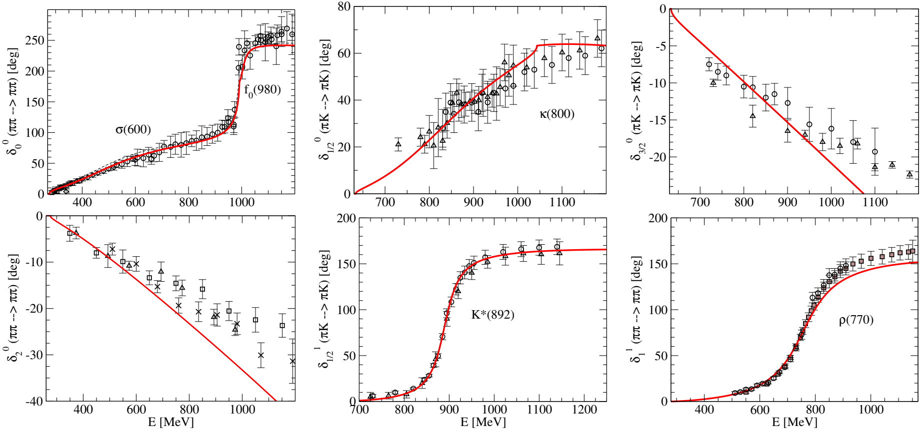

Figure: Fit of the Low Energy Constants; solution ⟶ generates pseudo lattice data.

Unitarized Chiral Perturbation Theory in a finite volume: the $\kappa(800)$

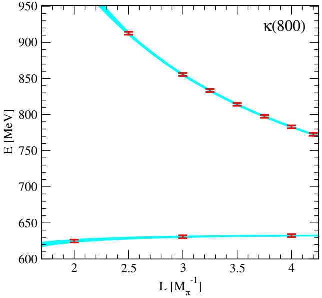

Figure: Pseudo lattice-data and (s^0, s^1, s^2) fit to those data with uncertainties (bands).

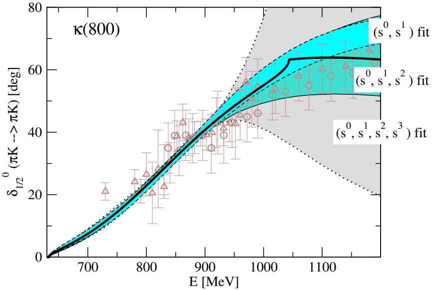

Figure: Solid line: Actual phase shift. Error bands of the (s^0, s^1), (s^0, s^1, s^2), and (s^0, s^1, s^2, s^3) fits.

Fit potential [$V_2 \equiv V_{\rm LO}$ known/fixed from f_π, f_K, f_η; $s \equiv E^2$]

$$V^{\rm fit} = \left(\frac{V_2 - V_4^{\rm fit}}{V_2^2}\right)^{-1}, \qquad V_4^{\rm fit} = a + b(s - s_0) + c(s - s_0)^2 + d(s - s_0)^3 + \cdots$$

[Actual errors twice as large from Gaussian distribution of centroids of data].

The $\kappa(800)$ pole

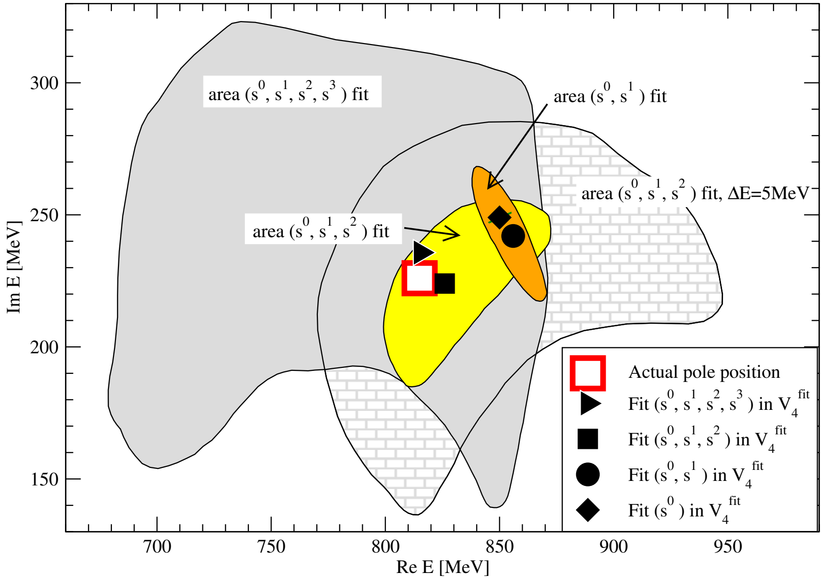

The P-wave resonances $K^*(892)$ and $\rho(770)$

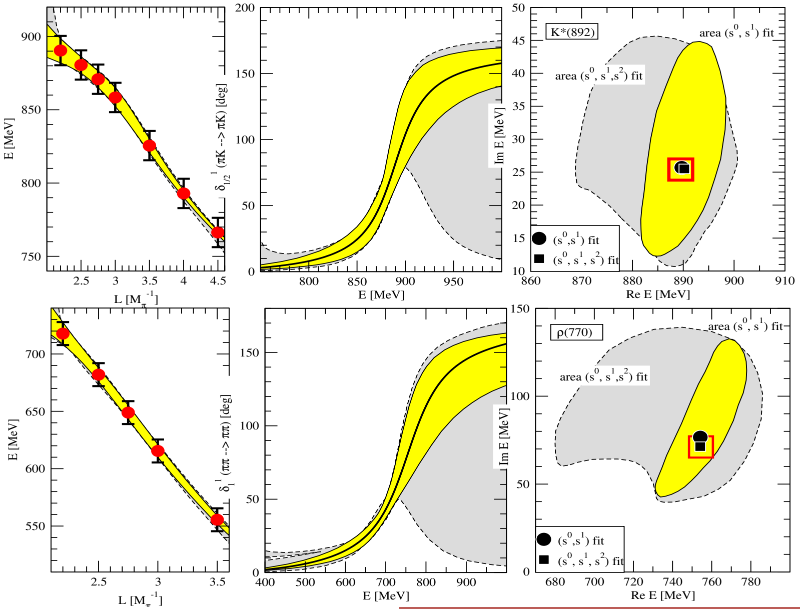

Residues

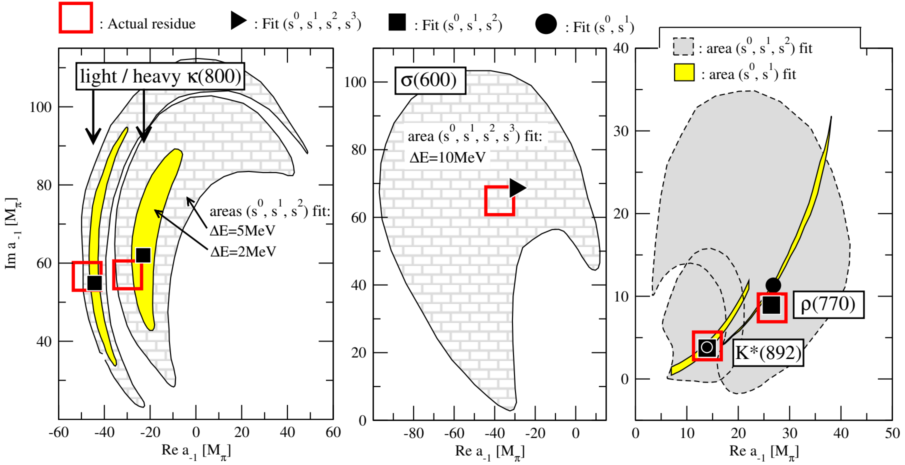
: Actual residue
: Fit (s0, s1, s2, s3)
: Fit (s0, s1, s2)
: Fit (s0, s1)
light / heavy κ(800)
areas (s0, s1, s2) fit:
ΔE=5MeV
ΔE=2MeV
Im a-1 [Mπ]
Re a-1 [Mπ]
σ(600)
area (s0, s1, s2, s3) fit:
ΔE=10MeV
: area (s0, s1, s2) fit
: area (s0, s1) fit
ρ(770)
K*(892)

Phase shifts from a moving frame

[M.D., Ulf-G. Meißner, E. Oset, A. Rusetsky, arXiv:1205.4838, accepted f. pub. in EPJA.]

- Lattice momenta in overall center-of-mass frame:

$$\vec{q}_\pi = \frac{2\pi}{L}\,\vec{n}, \quad \vec{n} \in \mathbb{Z}^3$$

- In meson-meson c.m. frame moving at $\vec{P}$:

$$\vec{q}_\pi^{\,*} = \Lambda_P(\vec{q}_\pi)$$

- Trick: Instead of changing L, obtain more eigenenergies from the same lattice by extracting lattice levels in a moving frame (Gottlieb-Rummukainen, 1995).
- Advantage: Computationally less demanding than varying L.
- Works bei
  - Davoudi & Savage (2011), Fu (2012), Leskovec & Prelovsek (2012), Dudek & Edwards & Thomas (2012), Hansen & Sharpe (2012), Briceño and Davoudi (2012),...

Mixing of partial waves

Example: S- and P-waves

- Infinite volume limit: Rotational symmetry

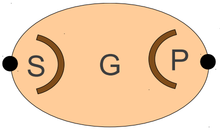

$$\int \frac{d^3\vec{q}}{(2\pi)^3}\, g(|\vec{q}|)\; Y_{\ell m}(\theta,\phi)\, Y^*_{\ell' m'}(\theta,\phi) \sim \delta_{\ell\ell'}\delta_{mm'}\,.$$

- Wigner-Eckart theorem:

S→S	0	0	0
0	$P_{-1} \to P_{-1}$	0	0
0	0	$P_0 \to P_0$	0
0	0	0	$P_1 \to P_1$

Mixing of partial waves

Example: S- and P-waves

- Infinite volume limit: Rotational symmetry

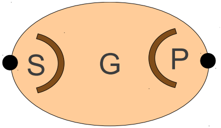

$$\int \frac{d^3\vec{q}}{(2\pi)^3}\, g(|\vec{q}|)\; Y_{\ell m}(\theta,\phi)\, Y^*_{\ell' m'}(\theta,\phi) \sim \delta_{\ell\ell'}\delta_{mm'}\,.$$

- Wigner-Eckart theorem:

S→S	0	0	0
0	P_{-1} → [illegible]	0	0
0	0	[illegible]	0
0	0	0	[illegible] → P_1

Equal

Mixing of partial waves

Example: S- and P-waves

- Finite volume: Rotational symmetry $\rightarrow$ Cubic symmetry

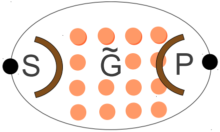

$$\frac{1}{L^3}\sum_{\vec{n}} g(|\vec{q}|)\, Y_{\ell m}(\theta,\phi)\, Y^*_{\ell' m'}(\theta,\phi) \sim A_{\ell\ell' m m'}\,.$$

- $S-G$-wave mixing, but $S-P$ waves still orthogonal:

S→S	0	0	0
0	$P_{-1} \rightarrow P_{-1}$	0	0
0	0	$P_0 \rightarrow P_0$	0
0	0	0	$P_1 \rightarrow P_1$

Breaking of cubic symmetry through boost

Example: Lattice points $\vec{q}^*$ boosted with $P = (0,0,0) \to \frac{2\pi}{L}(0,0,2)$:

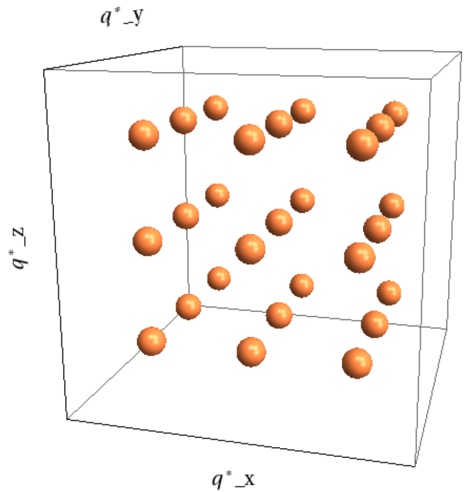

Mixing of partial waves

Example: S- and P-waves

- Finite volume & boost: Cubic symmetry $\to$ subgroups of cubic symmetry

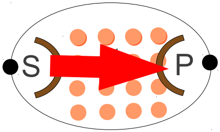

$$\frac{1}{L^3}\sum_{\vec{n}} g(|\vec{q}|)\, Y_{\ell m}(\theta,\phi)\, Y^*_{\ell' m'}(\theta,\phi) \sim A_{\ell\ell' m m'}\,.$$

- For boost $P = \frac{2\pi}{L}$ (0,1,1):

$S \to S$	0	$S \to P_0$	0
0	$P_{-1} \to P_{-1}$	0	$P_{-1} \to P_1$
$P_0 \to S$	0	$P_0 \to P_0$	0
0	$P_1 \to P_{-1}$	0	$P_1 \to P_1$

Mixing of partial waves

Example: S- and P-waves

- Finite volume & boost: Cubic symmetry → subgroups of cubic symmetry

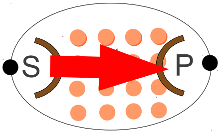

$$\frac{1}{L^3}\sum_{\vec{n}} g(|\vec{q}|)\, Y_{\ell m}(\theta,\phi)\, Y^*_{\ell' m'}(\theta,\phi) \sim A_{\ell\ell' mm'}\,.$$

- More complicated boosts:

S→S	S→P_{-1}	S→P_0	S→P_1
P_{-1}→S	P_{-1}→P_{-1}	P_{-1}→P_0	P_{-1}→P_1
P_0→S	P_0→P_{-1}	P_0→P_0	P_0→P_1
P_1→S	P_1→P_{-1}	P_1→P_0	P_1→P_1

Energy eigenvalues for different boosts: κ/K^*-system

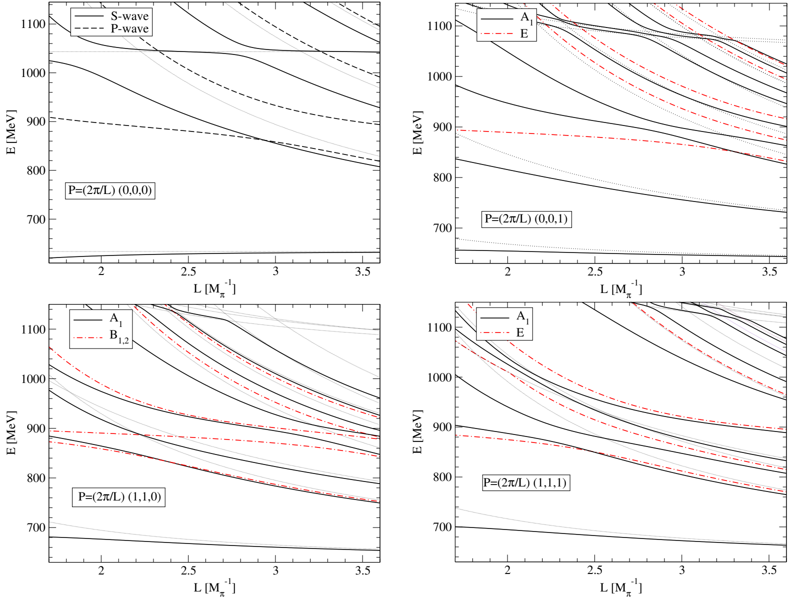

Disentanglement of partial waves

Example: S- and P-waves for the $\kappa(800)/K^*(892)$ system

Knowledge of P-wave (from separate analysis of lattice data) allows to disentangle the S-wave:

$$p\,\cot\delta_S = -8\pi\,E\,\frac{p\,\cot\delta_P\,\hat{G}_{SS} - 8\pi E(\hat{G}_{SP}^2 - \hat{G}_{SS}\hat{G}_{PP})}{p\,\cot\delta_P + 8\pi\,E\,\hat{G}_{PP}}$$

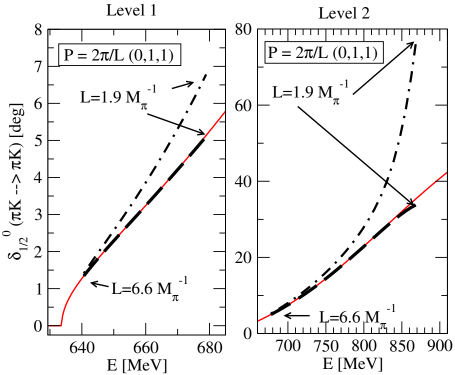

- $\delta_S \equiv \delta^0_{1/2}(\pi K \to \pi K)$
- Red solid: Actual S-wave phase shift.
- Dash-dotted: Reconstructed S-wave phase shift, PW-mixing ignored.
- Dashed: Reconstructed S-wave phase shift, PW-mixing disentangled.
- small p-wave: Level shift
  $$\Delta E \simeq -\frac{6\pi E_S \delta_P}{L^3 p\omega_1\omega_2}$$

Mixing of partial waves in boosted multiple channels: $\sigma(600)$

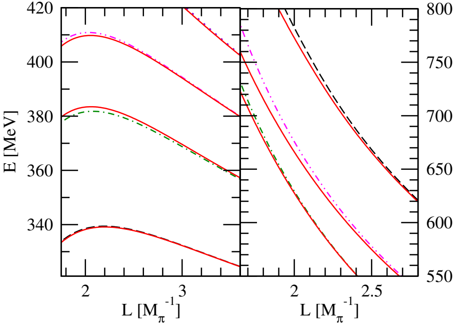

Solid: Levels from A_1^+.
Non-solid: Neglecting the D-wave.

- $\pi\pi$ & $\bar{K}K$ in S-wave, $\pi\pi$ in D-wave.
- Organization in Matrices (A_1^+), e.g. $\vec{P} = (2\pi/L)(0,0,1)$, $(2\pi/L)(1,1,1)$, and $(2\pi/L)(0,0,2)$:

$$V = \begin{pmatrix} V_S^{(11)} & V_S^{(12)} & 0 \\ V_S^{(21)} & V_S^{(22)} & 0 \\ 0 & 0 & V_D^{(22)} \end{pmatrix}$$

$$\tilde{G} = \begin{pmatrix} \tilde{G}^{R\,(1)}_{00,00} & 0 & 0 \\ 0 & \tilde{G}^{R\,(2)}_{00,00} & \tilde{G}^{R\,(2)}_{00,20} \\ 0 & \tilde{G}^{R\,(2)}_{20,00} & \tilde{G}^{R\,(2)}_{20,20} \end{pmatrix}$$

- Phase extraction (κ): Expand and fit V_S, V_P *simultaneously* to different representations instead of
  1. P-wave from B_1, B_2, E
  2. S-wave from P and A_1 (reduction of error).

Phase shifts from a moving frame: the $\sigma(600)$

Comparison: *Variation of L vs moving frames*

- The first two levels for the first five boosts:

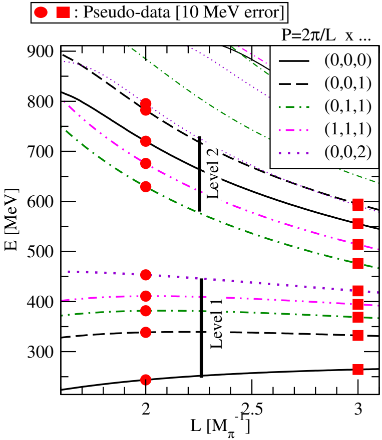

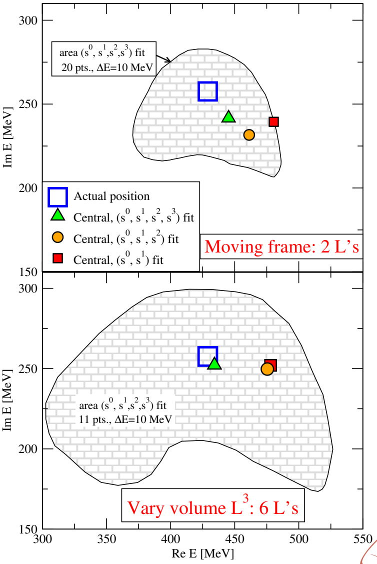

Twisting the boundary conditions (B.C.)

[Suganuma et. al. (2006), Bernard/Lage/Meißner/Rusetsky (2011), M.D./Meißner/Oset/Rusetsky (2011)]

- Periodic B.C.:
  $\Psi(\vec{x} + \hat{\mathbf{e}}_i L) = \Psi(\vec{x})$
- Periodic in 2 dim.:

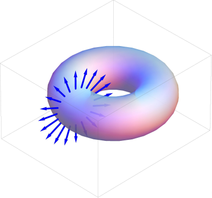

$\theta_1 = 0$

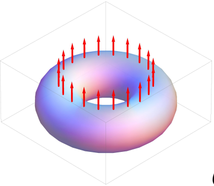

$\theta_2 = 0$

- Twisted B.C.:
  $\Psi(\vec{x} + \hat{\mathbf{e}}_i L) = e^{i\theta_i}\Psi(\vec{x})$
- Periodic/antiperiodic:

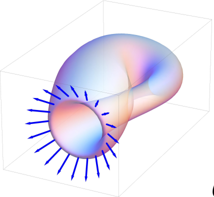

$\theta_1 = 0$

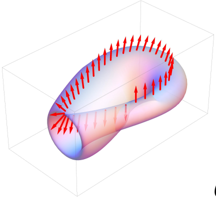

$\theta_2 = \pi$

[figs: thanks to M.Mai]

Example: the $f_0(980)$

- S-wave, coupled-channels $\pi\pi$, $\bar{K}K$.
- Twisted B.C. for the s-quark:
  $u(\vec{x} + \hat{\mathbf{e}}_i L) = u(\vec{x})$
  $d(\vec{x} + \hat{\mathbf{e}}_i L) = d(\vec{x})$
  $s\,(\vec{x} + \hat{\mathbf{e}}_i L) = e^{i\theta_i}\, s(\vec{x})$
- Three unknown potentials
  - $V(\pi\pi \to \pi\pi)$
  - $V(\pi\pi \to \bar{K}K)$
  - $V(\bar{K}K \to \bar{K}K)$

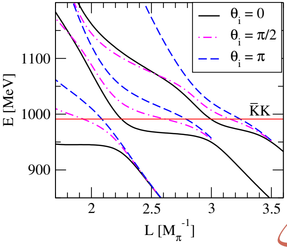

Disentangling coupled channels (the strict but impossible scenario)

Three measurements at the same E requires tuning of L

Asymmetric boxes

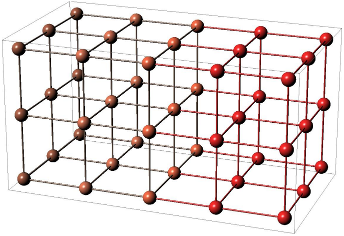

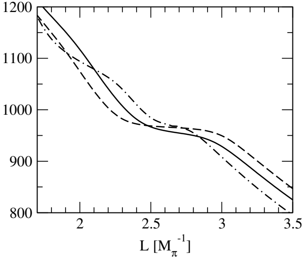

- $L_x = L, L_y = L, L_z = x\,L$, where $x = 0.6$ (solid lines), $x = 1.0$ (dashed lines), $x = 1.4$ (dash-dotted lines)

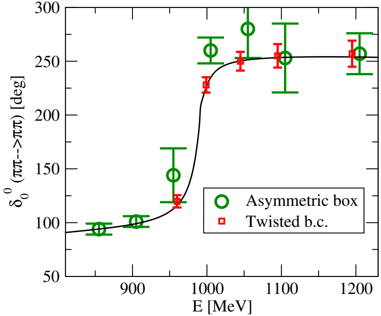

Reconstruction of the infinite volume limit (twisted boundary conditions)

[M.D./Meißner/Oset/Rusetsky, EPJA **47** (2011)]

- Expand the two-channel potential: $V_{ij} = a_{ij} + b_{ij}(s - 4M_K^2)$, i, j: $\pi\pi$, $\bar{K}K$.

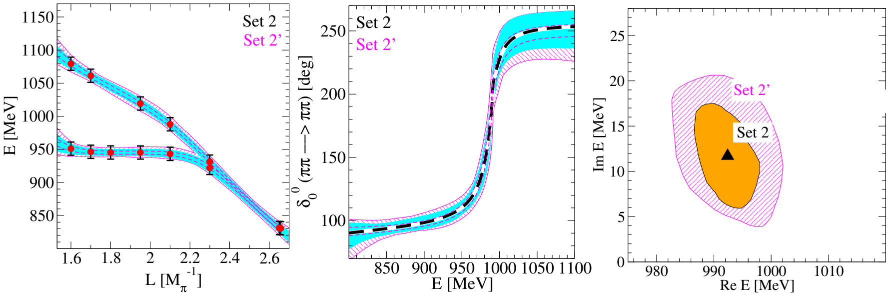

Left: pseudo-data (periodic & anti-periodic B.C.).
Center: Extracted phase with uncertainty.
Right: Extracted $f_0(980)$ pole with uncertainty.

Resonances vs. inelastic thresholds [$f_0(980)$]

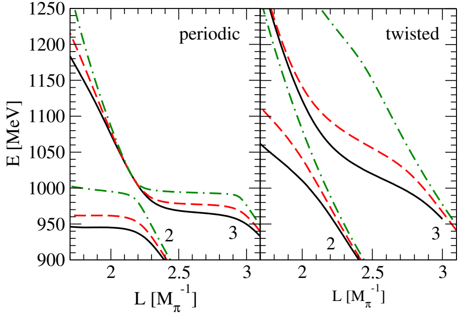

Levels

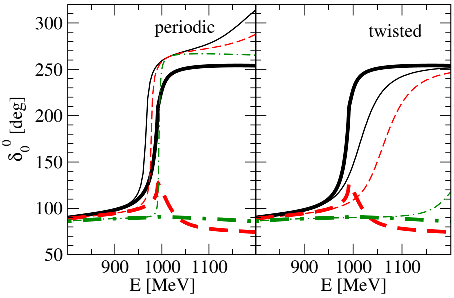

Pseudo-phases

→ No qualitative change in levels when removing resonance.

→ Ignoring the channel opening, always a resonance is seen (whether it is there or not).

The $N^*(1535)/N^*(1650)$ and hidden strangeness

LO+Res.: [M.D., K. Nakayama, EPJA 43 (2010)], NLO: [P.C. Bruns, M. Mai, U.-G. Meißner, PLB 697 (2011)].

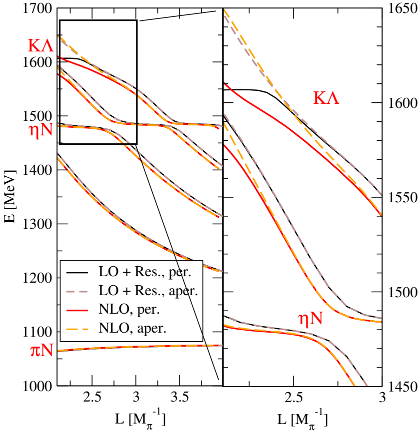

- LO+Res.: $N^*(1535)$ as $K\Lambda$, $K\Sigma$ quasi-bound state; genuine $N^*(1650)$.
- NLO: $N^*(1535)$ & 1650 as $K\Lambda$, $K\Sigma$ quasi-bound states.
- Hidden strangeness through antiperiodic boundary condition for the strange quark.
- Level spectrum dominated by thresholds in both scenarios.

Three-body effects: the $a_1(1260)$ [see also E. Oset, L. Roca, PRD 85 (2012)]

new lattice data: S. Prelovsek, C.B. Lang, D. Mohler, M. Vidmar, PoS LATTICE2011 (2011) 137

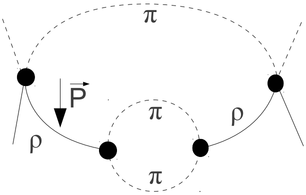

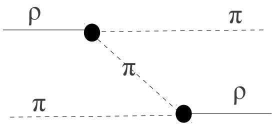

Boosted $\pi\pi$ self energy:

$$\tilde{\Pi}_{\lambda\lambda} = J\,\frac{4\pi}{3}\,\frac{1}{L^3}\sum_{\vec{n}}(q^*)^2\;Y_{1\lambda}(\theta_{q^*},\phi_{q^*}) \times Y^*_{1\lambda'}(\theta_{q^*},\phi_{q^*})\,f(q^*)$$

3×3 self energy:

$$\tilde{\Pi} = \begin{pmatrix} \tilde{\Pi}_{1,1} & \tilde{\Pi}_{1,0} & \tilde{\Pi}_{1,-1} \\ \tilde{\Pi}_{0,1} & \tilde{\Pi}_{0,0} & \tilde{\Pi}_{0,-1} \\ \tilde{\Pi}_{-1,1} & \tilde{\Pi}_{-1,0} & \tilde{\Pi}_{-1,-1} \end{pmatrix},$$

Dressed propagator

$$\tilde{S}^D_{\pi\rho} = \frac{1}{2\omega_1}\left((S^B_{\pi\rho}\,\mathbb{1})^{-1} - \tilde{\Pi}\right)^{-1}$$

Sum over boosts $\vec{P}$:

$$\tilde{G}_{\pi\rho} = \frac{1}{L^3}\sum_{\vec{P}}\tilde{S}^D_{\pi\rho}\ .$$

$\pi\rho$ scattering equation:

$$\tilde{T}_{\pi\rho} = (\mathbb{1} - \hat{V}_{\pi\rho}\,\tilde{G}_{\pi\rho})^{-1}\,\hat{V}_{\pi\rho}, \quad \hat{V}_{\pi\rho} = V_{\pi\rho}\mathbb{1}$$

Lattice levels:

$$\det(\mathbb{1} - \hat{V}_{\pi\rho}\,\tilde{G}_{\pi\rho}) = 0\ .$$

(+ pion exchange, required from 3-body unitarity; certain 3-body singularities cancel [K. Polejaeva and A. Rusetsky, 1203.1241]).

Outlook πN & $\pi\pi N$: Coupled-channels, PW mixing, and three-body states
[M.D. et al., in preparation]

- Three particles in a finite volume: [K. Polejaeva and A. Rusetsky, arXiv:1203.1241]
- Coupled-channel, pseudo two-particle formalism:

i_c	$J^P =$	$J=1/2$		$J=3/2$		$J=5/2$	
		$\frac{1}{2}^-$	$\frac{1}{2}^+$	$\frac{3}{2}^+$	$\frac{3}{2}^-$	$\frac{5}{2}^-$	$\frac{5}{2}^+$
1	πN	S11	P11	P13	D13	D15	F15
2	$\rho N(S=1/2)$	S11	P11	P13	D13	D15	F15
3	$\rho N_{(S=3/2,\lvert J-\ell\rvert=1/2)}$	—	P11	P13	D13	D15	F15
4	$\rho N_{(S=3/2,\lvert J-\ell\rvert=3/2)}$	D11	—	F13	S13	G15	P15
5	ηN	S11	P11	P13	D13	D15	F15
6	$\pi\Delta(\lvert J-\ell\rvert=1/2)$	—	P11	P13	D13	D15	F15
7	$\pi\Delta(\lvert J-\ell\rvert=3/2)$	D11	—	F13	S13	G15	P15
8	σN	P11	S11	D13	P13	F15	D15
9	$K\Lambda$	S11	P11	P13	D13	D15	F15
10	$K\Sigma$	S11	P11	P13	D13	D15	F15

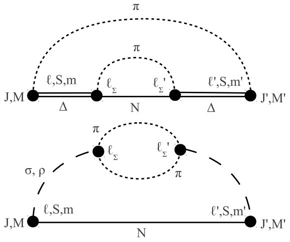

Figure: Intermediate $\pi\pi N$ states and their couplings. Above: $\pi\Delta$. Below: σN, ρN. The self energy insertions are resummed.

- space of lattice point $\otimes$ space of partial waves $\otimes$ space of third components $\otimes$ channel space
- Applications: Roper,... in the finite volume.

Analytic structure of the scattering amplitude: P11 in meson-baryon

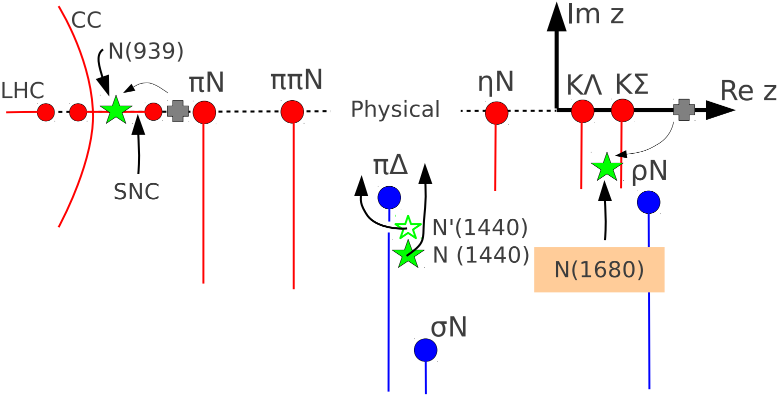

[D. Rönchen, M.D. *et al.*, in preparation, S. Ceci, M.D. *et al.*, PRC 84 (2011)]

Challenges for meson-baryon

For anything beyond the $\Delta(1232)$:

- $\pi\pi N$ known to be essential in πN.
- Coupled channels essential [$N^*(1535)$,...].
- MB:SG-wave, PF-wave, DG AND mixing of D-waves, D13 & D15. Additional mixing through different $\pi\pi N$ channels.
- Moving frames: All partial waves mix instantly; higher partial waves not necessarily small (F37,...).
- Parameterization of the transition kernels (MB) & (MMB):
  - GWU/SAID expansion in polynomials.
  - Dynamical coupled-channel approaches.

The $\Lambda(1405)$

[M. D./Haidenbauer/Meißner/Rusetsky, EPJA **47** (2011)]

- (Non-factorizing/off-shell) Lippman-Schwinger equation in the finite volume,

$$T^{(\mathrm{P})}(q'',q') = V(q'',q') + \frac{2\pi^2}{L^3}\sum_{i=0}^{\infty}\vartheta^{(\mathrm{P})}(i)\,\frac{V(q'',q_i)\,T^{(\mathrm{P})}(q_i,q')}{\sqrt{s}-E_a(q_i)-E_b(q_i)}, \quad q_i = \frac{2\pi}{L}\sqrt{i}\,.$$

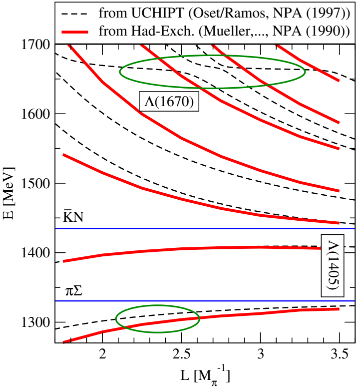

- Access to sub-$\bar{K}N$-threshold dynamics:
- Discrepancies of lowest levels: levels sensitive to different $\Lambda(1405)$ dynamics.
- One- or two-pole structure:
  - Will NOT lead to additional level.
  - but shifted threshold levels.

Summary

- $m_{\text{quark, lattice}} \to m_{\text{quark, physical}}$ in modern lattice simulations.
  → Resonances can decay on the lattice.
  → Finite volume effects dominate the resonance spectrum.
  → Resonances cannot be identified with individual levels.
  → inelastic S-wave thresholds have the same signature as resonances.

- Chiral Effective Field Theory allows to include model independent properties of the amplitude & to stabilize extraction of phases and resonances.

- Analysis tools:
  → Variation of the box size L vs. moving frames (partial wave mixing).
  → Multi-channel analysis, extension to three particles.
  → Twisted boundary conditions for the strange quark.

- Continuity assumptions on the amplitude allows for global level fit, should come with error analysis.

- Coupled-channels and three-particle states: more assumptions necessary if lattice data scarce (just like in analysis of experimental data).

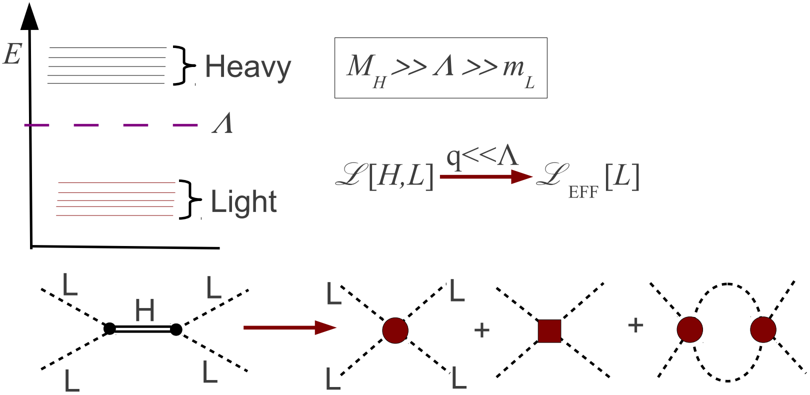

- Power counting: Systematic expansion in $\frac{q}{\Lambda_\chi}$, $\frac{M_\pi}{\Lambda_\chi}$.
- Idea: Chiral expansion of potential V; LO fixed term stabilizes extraction, LECs or other suitable expansion fitted to lattice levels.

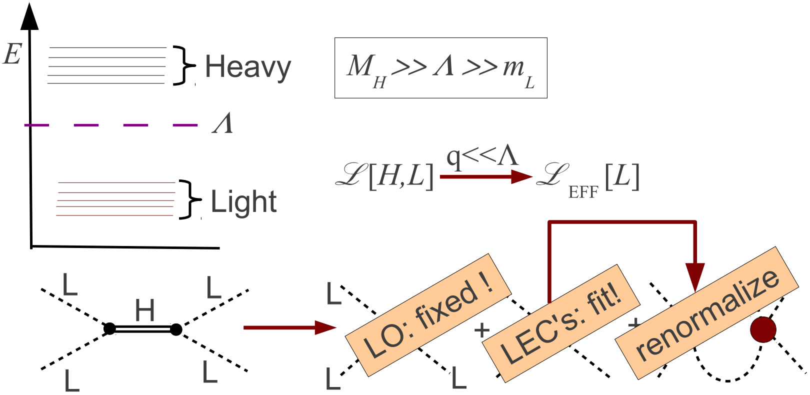

- Power counting: Systematic expansion in $\frac{q}{\Lambda_\chi}$, $\frac{M_\pi}{\Lambda_\chi}$.
- Idea: Chiral expansion of potential V; LO fixed term stabilizes extraction, LECs or other suitable expansion fitted to lattice levels.

Low-energy constants/poles

Table: Fitted values for the L_i [$\times 10^{-3}$] and $q_{\max}$ [MeV].

L_1	L_2	L_3	L_4
$0.873^{+0.017}_{-0.028}$	$0.627^{+0.028}_{-0.014}$	-3.5 [fixed]	$-0.710^{+0.022}_{-0.026}$
L_5	$L_6 + L_8$	L_7	$q_{\max}$ [MeV]
$2.937^{+0.048}_{-0.094}$	$1.386^{+0.026}_{-0.050}$	$0.749^{+0.106}_{-0.074}$	981 [fixed]

Table: Pole positions z_0 [MeV] and residues $a_{-1}[M_\pi]$ in different channels.
I, L, S: isospin, angular momentum, strangeness.

I	L	S	Resonance	sheet	z_0 [MeV]	a_{-1} $[M_\pi]$	a_{-1} $[M_\pi]$
0	0	0	$\sigma(600)$	pu	$434+i\,261$	$-31-i\,19\,(\bar{K}K)$	$-30+i\,86\,(\pi\pi)$
0	0	0	$f_0(980)$	pu	$1003+i\,15$	$16-i\,79\,(\bar{K}K)$	$-12+i\,4\,(\pi\pi)$
1/2	0	-1	$\kappa(800)$	pu	$815+i\,226$	$-36+i\,39\,(\eta K)$	$-30+i\,57\,(\pi K)$
1	0	0	$a_0(980)$	pu	$1019-i\,4$	$-10-i\,107\,(\bar{K}K)$	$21-i\,31\,(\pi\eta)$
0	1	0	$\phi(1020)$	p	$976+i\,0$	$-2+i\,0\,(\bar{K}K)$	—
1/2	1	-1	$K^*(892)$	pu	$889+i\,25$	$-10+i\,0.1\,(\eta K)$	$14+i\,4\,(\pi K)$
1	1	0	$\rho(770)$	pu	$755+i\,95$	$-11+i\,2\,(\bar{K}K)$	$33+i\,17\,(\pi\pi)$

- Unitarity: $T = [\text{Re}\, T^{-1} - i\,\sigma]^{-1}$; σ: diagonal phase space matrix.
- Use up to $\mathcal{O}(p^4)$ terms to approximate the inverse amplitude $\text{Re}\, T^{-1}$.
- Not a full one-loop calculation.
- Final result for the T-matrix:

$$T = V_2\,(V_2 - V_4 - V_2\,G\,V_2)^{-1}\,V_2 \qquad (1)$$

V_2: Leading order; V_4: NLO-order polynomial terms; G: propagator matrix in coupled channels.

- A genuine resonance (unitary):

$$T = \frac{ap^2}{q^2 - M^2 + 2\,M\,i\,\Gamma}, \quad 2m\Gamma = -a\,p^2\,\text{Im}\,G\,. \qquad (2)$$

To order $\mathcal{O}(k^2)$ and $\mathcal{O}(k^4)$ $[k \equiv p, q]$:

$$V_2 = -a\frac{p^2}{M^2}, \quad \text{Re}\,V_4 = -\frac{ap^2\,q^2}{M^4} = \frac{V_2\,q^2}{M^2}.$$

Insert this in Eq. (1) $\rightarrow$ Eq. (2).

Case of a low $\kappa(800)$ pole

Refit to Roy-Steiner solution of [Descotes/Moussallam, EPJC48 (2006)].

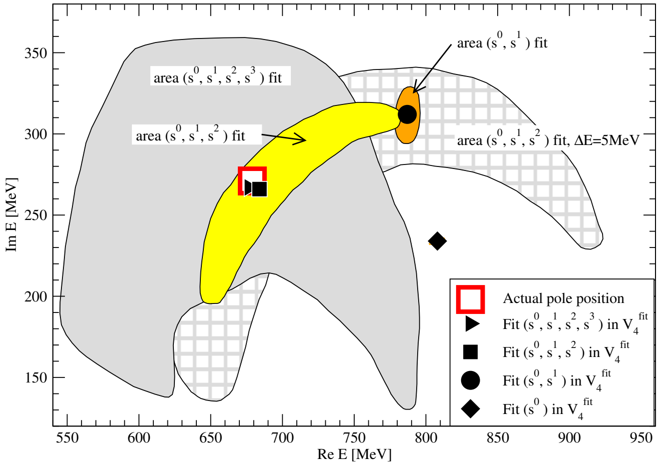

Figure: Case of a low $\kappa(800)$ pole. Pole positions of the κ (central values) together with uncertainty areas, from fits to pseudo lattice-data.

$$\langle L'S'k'|T^{IJ}_{\mu\nu}|LSk\rangle = \langle L'S'k'|V^{IJ}_{\mu\nu}|LSk\rangle$$

$$+\sum_{\gamma, L''S''}\int_0^\infty k''^2\, dk''\langle L'S'k'|V^{IJ}_{\mu\gamma}|L''S''k''\rangle\, G(k'')\,\langle L''S''k''|T^{IJ}_{\gamma\nu}|LSk\rangle$$

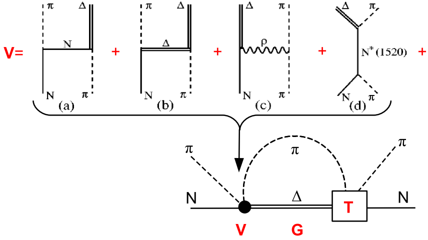

$\pi N \to \pi N$ [NPA **829** (2009)]

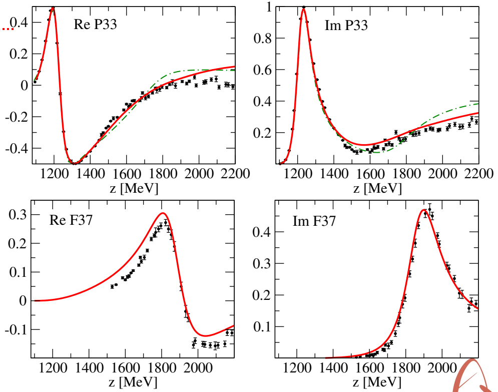

- Hadron exchange.
- Full analyticity (dispersive parts).
- All partial waves are linked (t-, u-channel processes)
- Channels linked (SU(3) symmetry).

A model for the meson-baryon dynamics

Comprehensive analysis of $\gamma N/\pi N \to \pi N, \eta N, KY$ [Jülich, Georgia, Washington]

$$\langle L'S'k'|T^{IJ}_{\mu\nu}|LSk\rangle = \langle L'S'k'|V^{IJ}_{\mu\nu}|LSk\rangle + \sum_{\gamma,L''S''}\int_0^\infty k''^2\,dk''\,\langle L'S'k'|V^{IJ}_{\mu\gamma}|L''S''k''\rangle\; G(k'')\;\langle L''S''k''|T^{IJ}_{\gamma\nu}|LSk\rangle$$

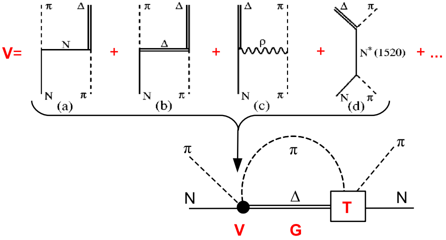

- Hadron exchange.
- Full analyticity (dispersive parts).
- All partial waves are linked (t-, u-channel processes)
- Channels linked (SU(3) symmetry).

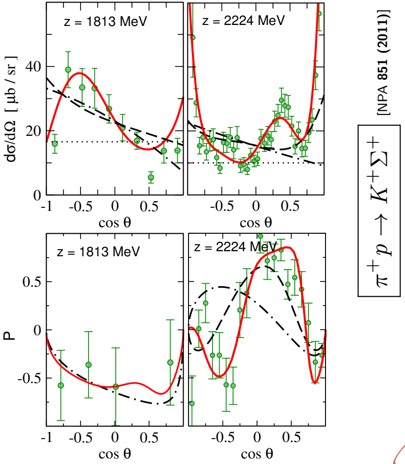

A model for the meson-baryon dynamics

Comprehensive analysis of $\gamma N/\pi N \to \pi N, \eta N, KY$ [Jülich, Georgia, Washington]

$$\langle L'S'k'|T^{IJ}_{\mu\nu}|LSk\rangle = \langle L'S'k'|V^{IJ}_{\mu\nu}|LSk\rangle$$
$$+ \sum_{\gamma, L''S''} \int_0^\infty k''^2\, dk'' \langle L'S'k'|V^{IJ}_{\mu\gamma}|L''S''k''\rangle\, G(k'')\, \langle L''S''k''|T^{IJ}_{\gamma\nu}|LSk\rangle$$

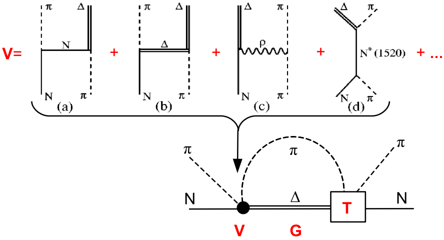

$\gamma N \to \pi N$ [F. Huang, M.D., et al., PRC 85, 2012]

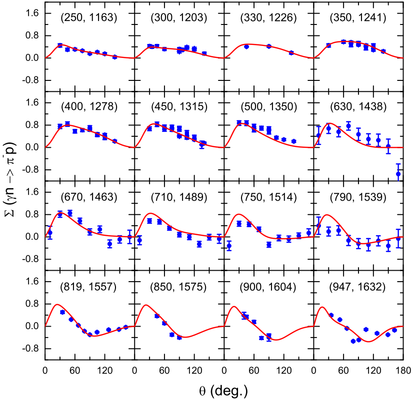

- Hadron exchange.
- Full analyticity (dispersive parts).
- All partial waves are linked (t-, u-channel processes)
- Channels linked (SU(3) symmetry).